Stanley, J.R., and Flowers, R.M., 2023, Localized Cenozoic erosion on the southern African Plateau: A signal of topographic uplift?: Geology, https://doi.org/10.1130/G50790.1.

Supplemental Material

METHODS DETAIL

To generate the predicted date-eU relationships in Figures 2 and 3, we input a range of tT paths into the modeling software QTQt (Gallagher, 2012). The simulations use a model for the expected behavior of He diffusion in apatite taking into account the accumulation of radiation damage in the crystal to calculate the expected AHe date for the input tT path. In this case we used the Radiation Damage Accumulation and Annealing Model (RDAAM, Flowers et al., 2009). Some forward models were also run in the HeFTy software program (Ketcham, 2005) and yielded nearly identical results as expected because both programs use RDAAM to predict the dates from the forward models. The two software programs have different inverse modeling philosophies, sometimes resulting in different solutions when trying to find the best fitting tT paths for a given dataset (e.g., Vermeesch and Tian, 2014), but in this case we are only using the forward modeling capabilities so the choice of software program does not affect our results. The predictions are made for a generic grain with 50 µm equivalent spherical radius, similar to the average of our dataset, and using a range of eU from 1 to 150 ppm.

The selection of the tT paths to test (Table S2) was based on our previous work on these kimberlites and their eruption ages (Stanley et al., 2013, 2015; Stanley and Flowers, 2020). Previously we ran inverse models to find good-fitting thermal histories for individual samples, which we generalized here. Kimberlites that erupted in the Early Cretaceous generally experienced a cooling pulse around the time of eruption, represented by the major cooling phase we input at 120-115 Ma (Table S2, solid lines Fig 2C, 3C, 3F). Kimberlites that erupted in the Late Cretaceous also generally experienced cooling around their eruption time, as did one pipe (New Elands) that was emplaced earlier but underwent Late Cretaceous cooling (Stanley et al., 2015). The cooling phase of these pipes is represented by substantial cooling in the forward model at 95-90 Ma (Table S2, dashed lines Fig 2C, 3C, 3F). The magnitude of Cenozoic cooling (Fig 3F) was chosen based on the range of Cenozoic cooling seen in good-fit paths from inverse tT models of individual samples with strong date-eU correlations (Stanley et al., 2013; 2015; Stanley and Flowers 2020). The timing of Cenozoic cooling was chosen to test a range of times for the cooling phase, but specific paths correspond to proposed mechanisms (Table S2, Fig 3C). The 35-30 Ma timing could represent rock uplift and associated erosion due to upper mantle convection when the African plate became stationary with respect to the underlying mantle (Burke, 1996). The 15-13 Ma timing roughly corresponds to the mid-Miocene Climatic Optimum (Zachos et al., 2001) when climate change and increased precipitation could have enhanced erosion on the plateau (see main text for additional discussion). The 5-1 Ma timing could represent recent rock uplift due to upper mantle processes (e.g., Partridge and Maud, 1987). Using these tT paths we are able to model the predicted AHe dates for a wide range of possible Cenozoic cooling Scenarios (Fig 3).

REFERENCES

Burke, K., 1996, The african plate: South african journal of geology, v. 99, p. 341–409.

Flowers, R.M., Ketcham, R.A., Shuster, D.L., and Farley, K.A., 2009, Apatite (U–Th)/He thermochronometry using a radiation damage accumulation and annealing model: Geochimica et Cosmochimica acta, v. 73, p. 2347–2365, doi:10/ffkmvz.

Gallagher, K., 2012, Transdimensional inverse thermal history modeling for quantitative thermochronology: Journal of Geophysical Research: Solid Earth, v. 117, doi:10/fztzrw.

Ketcham, R.A., 2005, Forward and inverse modeling of low-temperature thermochronometry data: Reviews in mineralogy and geochemistry, v. 58, p. 275–314.

Partridge, T.C., and Maud, R.R., 1987, Geomorphic evolution of southern Africa since the Mesozoic: South African Journal of Geology, v. 90, p. 179–208.

Stanley, J.R., and Flowers, R.M., 2020, Mesozoic denudation history of the lower Orange River and eastward migration of erosion across the southern African Plateau: Lithosphere, doi:10/ggjt45.

Stanley, J.R., Flowers, R.M., and Bell, D.R., 2015, Erosion patterns and mantle sources of topographic change across the southern African Plateau derived from the shallow and deep records of kimberlites: Geochemistry, Geophysics, Geosystems, v. 16, p. 3235–3256, doi:10/f7zgxb.

Stanley, J.R., Flowers, R.M., and Bell, D.R., 2013, Kimberlite (U-Th)/He dating links surface erosion with lithospheric heating, thinning, and metasomatism in the southern African Plateau: Geology, v. 41, p. 1243–1246, doi:10/f5pbr9.

Vermeesch, P., and Tian, Y., 2014, Thermal history modelling: HeFTy vs. QTQt: Earth-Science Reviews, v. 139, p. 279–290, doi:10.1016/j.earscirev.2014.09.010.

Zachos, J., Pagani, M., Sloan, L., Thomas, E., and Billups, K., 2001, Trends, Rhythms, and Aberrations in Global Climate 65 Ma to Present: Science, v. 292, p. 686–693, doi:10.1126/science.1059412.

Figure S1. AHe date vs eU plots for all kimberlites included in the study. Colors as in Figure 1 with orange indicating a positive date-eU correlation, purple indicating no date-eU correlation, and grey indicating no grains <15ppm eU. Circles are pipes erupted >110 Ma while triangles are samples in the <110 Ma group in Figures 2 and 3.

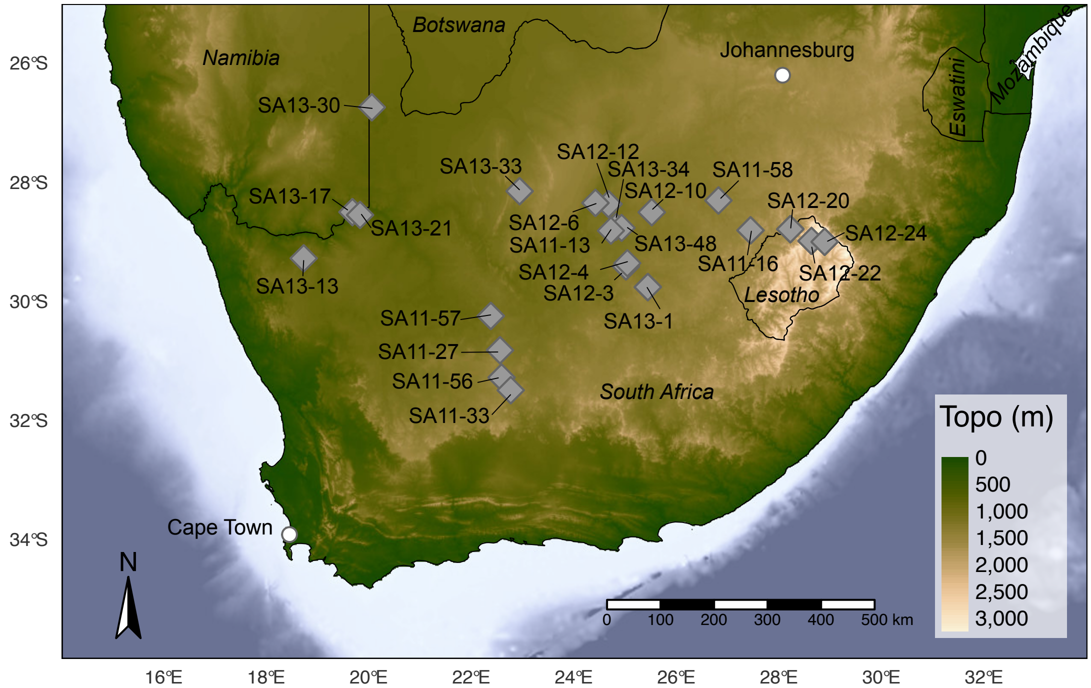

Figure S2. Sample locations for all samples included in the study.